Int. J. Heat Mass Transfer. Vol. 34, No. 6, pp. 1327–1336, 1991
Printed in Great Britain

0017–9310/91 $3.00 + 0.00

Natural convection near a vertical corner of an arbitrary angle

MAN HOE KIM,† MOON-UHN KIM‡ and DO HYUNG CHOI†

† Department of Mechanical Engineering, Korea Advanced Institute of Science and Technology, P.O. Box 150, Cheongryang, Seoul, Korea

‡ Department of Applied Mathematics, Korea Advanced Institute of Science and Technology, P.O. Box 150, Cheongryang, Seoul, Korea

(*Received* 28 *November* 1988)

Abstract—The laminar natural-convection heat transfer near a vertical corner of an arbitrary angle is presented. For large Grashof numbers, the corner-layer equations and appropriate boundary conditions are formulated in an oblique coordinate system based on the method of matched asymptotic expansions. The analysis is valid for any corner angles except the limiting angles 0° and 360°. The velocity and temperature distributions are numerically determined using the finite difference technique of ADI type for corner angles ranging from 60° to 300° for Prandtl numbers of 0.72 and 7.0.

1. INTRODUCTION

ONE OF the fundamental problems in natural convection is the buoyancy-driven flow from the surfaces composed of simple bodies such as flat plates and cylinders. The heat transfer characteristics of the combination bodies are quite different from those of the individual bodies due to the mutual interaction of the boundary layers. Because of these characteristics and the importance in practical applications, the natural convection boundary-layer interaction problem has attracted many investigators.

As for the two-dimensional flow, the subject has been studied extensively for various geometries [1–4]. On the other hand, the literature on the three-dimensional natural-convection boundary-layer flow still remains scanty. Liu and Guerra [5] studied theoretically the natural convection near the vertical corner of an arbitrary angle in a saturated porous medium and examined the interaction between the two plates. The laminar natural-convection boundary layer along a vertical rectangular corner was analysed in ref. [6]. For large Grashof numbers, corner-layer equations were derived and the interaction of the boundary layers and the features of the crossflow patterns which are very different from those of the high-Reynolds number flow along a 90° corner were discussed in refs. [7, 8].

As a generalization of the earlier work [6], the present study considers the laminar free convection along a vertical corner of an arbitrary angle, which is formed by two quarter-infinite rigid plates with coplanar leading edges. The vertical plates are kept at a uniform temperature T_w different from the ambient temperature T_∞ (it is assumed that $T_w > T_\infty$). For large Grashof number, the corner-layer equations and the boundary conditions are derived by a method similar to that used in ref. [9], which is concerned with the high-Reynolds-number flow in a streamwise corner of arbitrary angle.

2. CORNER-LAYER EQUATIONS

We consider the laminar natural-convection flow along the corner formed by the intersection of two vertical quarter-infinite plates. A suitable frame of reference for this problem is a non-orthogonal oblique coordinate system (x_0, y_0, z_0) depicted in Fig. 1. The origin is in the symmetry plane at the leading edge and the x_0 axis coincides with the intersection. Both y_0 and z_0 axes are perpendicular to the x_0 axis and lie, respectively, in the symmetry plane and in one of the joining quarter-infinite plates. The coordinates are simply related to the Cartesian coordinates x, y and z (see Fig. 1) by

$$(x_0, y_0, z_0) = (x, y - z\tan\alpha, z/\cos\alpha). \quad (1)$$

Invoking the Boussinesq approximation and neglecting the viscous dissipation in the fluid, the governing equations, namely, the continuity, Navier–Stokes, and energy equations, are given by

$$\frac{\partial u_0^*}{\partial x_0} + \frac{\partial v_0^*}{\partial y_0} + \frac{\partial w_0^*}{\partial z_0} = 0 \quad (2a)$$

$$\frac{Du_0^*}{Dt} = -\frac{1}{\rho}\frac{\partial p_0^*}{\partial x_0} + \nu\nabla^{*2}u_0^* + g\beta(T - T_\infty) \quad (2b)$$

$$\frac{D}{Dt}(v_0^* + w_0^*\sin\alpha) = -\frac{1}{\rho}\frac{\partial p_0^*}{\partial y_0} + \nu\nabla^{*2}(v_0^* + w_0^*\sin\alpha) \quad (2c)$$

$$\frac{D}{Dt}(w_0^* + v_0^*\sin\alpha) = -\frac{1}{\rho}\frac{\partial p_0^*}{\partial z_0} + \nu\nabla^{*2}(w_0^* + v_0^*\sin\alpha) \quad (2d)$$

$$\frac{DT}{Dt} = \kappa\nabla^{*2}T \quad (2e)$$

NOMENCLATURE

a grid spacing parameter, 0.2
Gr local Grashof number, $g\beta\Delta Tx^3/\nu^2$
H mesh size, 0.02
N, S transformed independent variables
Nu local Nusselt number
p_0^* pressure in x_0, y_0, z_0 coordinate system
p pressure in ξ, η, ζ coordinate system
Pr Prandtl number, ν/κ
r magnitude of scaled crossflow velocity, $(1/U_c)(Gr/4)^{1/4}(v^{*2}+w^{*2})^{1/2}$
T temperature
T_w wall temperature
T_∞ ambient temperature
ΔT temperature difference, $T_w - T_\infty$
u_0^*, v_0^*, w_0^* velocity components in the x_0, y_0, z_0 directions
u^*, v^*, w^* velocity components in the x, y, z directions
u, v, w scaled velocity components in the ξ, η, ζ directions
U_c convective velocity, $\frac{1}{2}(g\beta\Delta Tx)^{1/2}$
x_0, y_0, z_0 oblique coordinate system defined in Fig. 1
x, y, z Cartesian coordinate system.

Greek symbols
α $\frac{1}{2}(\pi - \alpha_c)$
α_c corner angle
β thermal expansion coefficient
γ $\lim_{\eta\to\infty}[-3f(\eta)]$
θ dimensionless temperature, $(T-T_\infty)/(T_w-T_\infty)$
κ thermal diffusivity
μ dynamic viscosity
ν kinematic viscosity, μ/ρ
ξ, η, ζ scaled independent variables
ρ density of fluid
τ_w wall shear stress
$\tau_{w,\infty}$ wall shear stress as $\zeta \to \infty$
ϕ, ψ velocity potential defined in equations (5)
Ω modified vorticity defined in equations (5).

where

$$\frac{\mathrm{D}}{\mathrm{D}t} \equiv u_0^* \frac{\partial}{\partial x_0} + v_0^* \frac{\partial}{\partial y_0} + w_0^* \frac{\partial}{\partial z_0}$$

$$\nabla^{*2} \equiv \frac{\partial^2}{\partial x_0^2} + \frac{1}{\cos^2\alpha}\left(\frac{\partial^2}{\partial y_0^2} - 2\sin\alpha\,\frac{\partial^2}{\partial y_0 \partial z_0} + \frac{\partial^2}{\partial z_0^2}\right).$$

Let us now introduce the following scaled dimensionless variables:

$$[u(\eta,\zeta), v(\eta,\zeta), w(\eta,\zeta)] = \left[\frac{u_0^*}{U_c}, \frac{v_0^*}{U_c}\left(\frac{Gr}{4}\right)^{1/4}, \frac{w_0^*}{U_c}\left(\frac{Gr}{4}\right)^{1/4}\right]$$

$$p(\eta,\zeta) = \frac{p_0^*}{\rho U_c^2}\left(\frac{Gr}{4}\right)^{1/2}$$

$$\theta(\eta,\zeta) = (T-T_\infty)/(T_w-T_\infty)$$

$$\eta = \frac{y_0}{x_0}\left(\frac{Gr}{4}\right)^{1/4}, \quad \zeta = \frac{z_0}{x_0}\left(\frac{Gr}{4}\right)^{1/4} \tag{3}$$

where Gr and U_c denote, respectively, the Grashof number and the convective velocity

$$Gr = g\beta\Delta Tx^3/\nu^2$$

$$U_c = \tfrac{1}{2}(g\beta\Delta Tx)^{1/2}.$$

For $Gr \gg 1$, substituting equations (3) into equations (2) and retaining the leading order terms in each equation give the following corner-layer equations:

$$-\tfrac{1}{4}(\eta u_\eta + \zeta u_\zeta - 2u) + v_\eta + w_\zeta = 0 \tag{4a}$$

$$-\frac{u}{4}(\eta u_\eta + \zeta u_\zeta - 2u) + v u_\eta + w u_\zeta = \bar{\nabla}^2 u + 4\theta \tag{4b}$$

$$-\frac{u}{4}(\eta\bar{v}_\eta + \zeta\bar{v}_\zeta + \bar{v}) + v\bar{v}_\eta + w\bar{v}_\zeta = -p_\eta + \bar{\nabla}^2\bar{v} \tag{4c}$$

$$-\frac{u}{4}(\eta\bar{w}_\eta + \zeta\bar{w}_\zeta + \bar{w}) + v\bar{w}_\eta + w\bar{w}_\zeta = -p_\zeta + \bar{\nabla}^2\bar{w} \tag{4d}$$

$$-\frac{u}{4}(\eta\theta_\eta + \zeta\theta_\zeta) + v\theta_\eta + w\theta_\zeta = \frac{1}{Pr}\bar{\nabla}^2\theta \tag{4e}$$

where

$$\bar{v} \equiv v + w\sin\alpha, \quad \bar{w} \equiv w + v\sin\alpha$$

$$\bar{\nabla} \equiv \frac{1}{\cos^2\alpha}\left(\frac{\partial^2}{\partial\eta^2} - 2\sin\alpha\,\frac{\partial^2}{\partial\eta\partial\zeta} + \frac{\partial^2}{\partial\zeta^2}\right).$$

After eliminating the pressure term between equations (4c) and (4d), the set of equations (4) may be written in a more convenient form in terms of 'the velocity potentials', ϕ and ψ, and 'the modified vorticity' Ω defined by

$$\phi = \left(\frac{\eta u}{4} - v\right)\cos\alpha, \quad \psi = \left(\frac{\zeta u}{4} - w\right)\cos\alpha$$

$$\Omega = \frac{1}{\cos^2\alpha}[(\psi_\eta - \phi_\zeta) + (\phi_\eta - \psi_\zeta)\sin\alpha]. \tag{5}$$

The final set of equations then takes the following form:

$$\nabla^2 u + \phi u_\eta + \psi u_\zeta - \frac{\cos\alpha}{2}u^2 + 4\theta\cos\alpha = 0$$

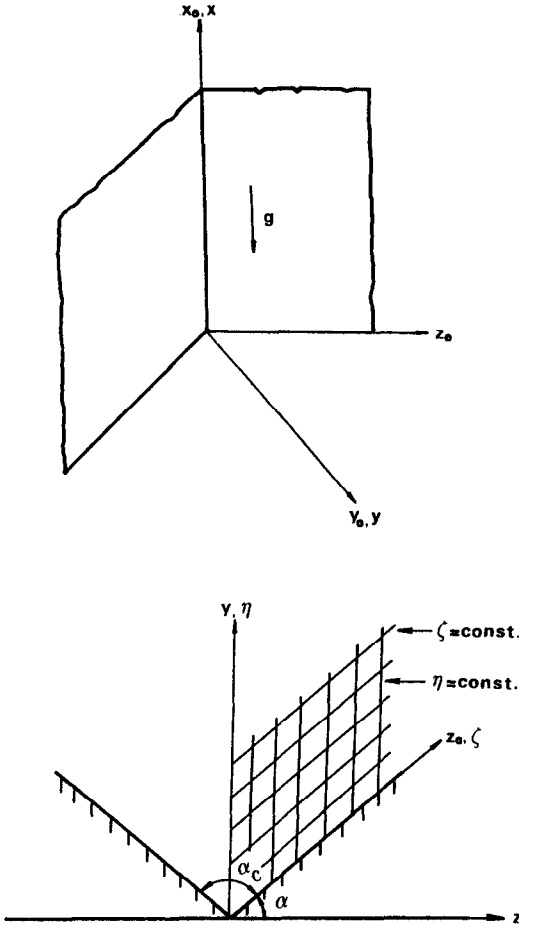

FIG. 1. Definition sketch.

$$\nabla^2\Omega+\phi\Omega_\eta+\psi\Omega_\zeta+u[\Omega\cos\alpha+\tfrac{3}{8}(\eta+\zeta\sin\alpha)u_\zeta$$

$$-\tfrac{3}{8}(\zeta+\eta\sin\alpha)u_\eta]+(\zeta+\eta\sin\alpha)\theta_\eta-(\eta+\zeta\sin\alpha)\theta_\zeta=0$$

$$\phi_{\eta\eta}-\phi_{\eta\zeta}\sin\alpha+\phi_{\zeta\zeta}+\psi_{\zeta\zeta}\sin\alpha$$

$$+\Omega_\zeta\cos^2\alpha-u_\eta\cos\alpha=0$$

$$\psi_{\eta\eta}-\psi_{\eta\zeta}\sin\alpha+\psi_{\zeta\zeta}+\phi_{\eta\eta}\sin\alpha$$

$$-\Omega_\eta\cos^2\alpha-u_\zeta\cos\alpha=0$$

$$\frac{1}{Pr}\nabla^2\theta+\phi\theta_\eta+\psi\theta_\zeta=0 \tag{6}$$

where

$$\nabla^2\equiv\frac{1}{\cos\alpha}\left(\frac{\partial^2}{\partial\eta^2}-2\sin\alpha\frac{\partial^2}{\partial\eta\partial\zeta}+\frac{\partial^2}{\partial\zeta^2}\right).$$

The corner-layer equations given above are of the elliptic type, and the solution is sought in the region $0\leqslant\eta,\zeta\leqslant\infty$.

3. BOUNDARY CONDITIONS

Since the governing equations are elliptic, the conditions are required on all four boundaries, i.e. $\eta=0$, $\zeta=0$, $\eta\to\infty$ and $\zeta\to\infty$.

3.1. *Conditions on the wall*, $\eta=0$

The uniform temperature condition is assumed along with the usual no-slip conditions at the wall, i.e.

$$u=\phi=\psi=0,\quad \Omega=\frac{1}{\cos^2\alpha}\psi_\eta,\quad \theta=1. \tag{7}$$

3.2. *Conditions on the symmetry plane*, $\zeta=0$

In the Cartesian coordinate system (x, y, z) (see Fig. 1), the velocity components u^* and v^* and the temperature T are symmetric with respect to z, while the component w^* is antisymmetric. Thus, on the symmetry plane $z=0$ (or $\zeta=0$)

$$\frac{\partial u^*}{\partial z}=\frac{\partial v^*}{\partial z}=w^*=\frac{\partial T}{\partial z}=0. \tag{8}$$

Condition (8) can be rewritten in terms of the corner-layer variables as

$$u_\zeta-u_\eta\sin\alpha=0,\quad \Omega=\psi=0$$

$$\phi_\zeta-(\phi_\eta-\psi_\zeta)\sin\alpha=0,\quad \theta_\zeta-\theta_\eta\sin\alpha=0. \tag{9}$$

3.3. *Conditions as* $\eta\to\infty$

As $\eta\to\infty$, the streamwise velocity component u and the temperature θ approach the values of zeroth-order potential flow, i.e.

$$u\sim 0,\theta\sim 0\quad \text{as } \eta\to\infty. \tag{10a}$$

It is evident that the crossflow components v and w are independent of η, as $\eta\to\infty$. In addition, from the continuity equation and irrotationality of the outer flow, it can be shown that v and w are independent of ζ also. That is, v and w become constants as $\eta\to\infty$. Moreover, since $w=0$ along $\zeta=0$, the plane of symmetry (see equation (8)), the limiting value of w should be 0. Equations (5) then give the conditions for the velocity potentials

$$\phi\sim-\gamma\cos\alpha,\psi\sim 0\quad \text{as } \eta\to\infty \tag{10b}$$

where the value of γ is the limiting value of v as $\eta\to\infty$ and will be determined in conjunction with the value of ϕ as $\zeta\to\infty$ (see Section 3.4). Finally, the irrotationality of the outer flow yields

$$\Omega\sim 0\quad \text{as } \eta\to\infty. \tag{10c}$$

3.4. *Conditions as* $\zeta\to\infty$

The asymptotic matching conditions can be determined by taking the limit of the corner-layer equations (6) as $\zeta\to\infty$ [10, 11]. Taking the results for the rectangular corner [6] into consideration, we formally assume that, for large ζ, the dependent variables take the following asymptotic form:

$$u\sim u_0(\eta)+u_1(\eta)/\zeta+\cdots$$

$$\Omega \sim \zeta\Omega_0(\eta)+\Omega_1(\eta)+\cdots$$
$$\phi \sim \phi_0(\eta)+\phi_1(\eta)/\zeta+\cdots$$
$$\psi \sim \zeta\psi_0(\eta)+\psi_1(\eta)+\cdots$$
$$\theta \sim \theta_0(\eta)+\theta_1(\eta)/\zeta+\cdots. \quad (11)$$

Substituting equations (11) into equations (6) and solving the resulting equations up to the second order, we obtain the appropriate matching conditions for the corner-layer variables:

$$u \sim 4f'(\eta)$$
$$\Omega \sim \zeta f''(\eta)/\cos\alpha+2f'(\eta)\tan\alpha+\psi_1'(\eta)/\cos^2\alpha$$
$$\phi \sim 3f(\eta)\cos\alpha$$
$$\psi \sim \zeta f'(\eta)\cos\alpha+\psi_1(\eta)$$
$$\theta \sim t(\eta). \quad (12)$$

Here $f(\eta)$ and $t(\eta)$ are the solutions for the natural-convection flow on the semi-infinite vertical flat plate, i.e.

$$f'''(\eta)+3f(\eta)f''(\eta)\cos^2\alpha - 2[f'(\eta)]^2\cos^2\alpha+t(\eta)\cos^2\alpha=0$$
$$t''(\eta)+3Pr\,f(\eta)t'(\eta)\cos^2\alpha=0$$
$$f(0)=f'(0)=0,\ t(0)=1 \quad \text{and} \quad f'(\infty)=t(\infty)=0 \quad (13)$$

and the equation for $\psi_1(\eta)$ is given by

$$\psi_1''(\eta)/\cos^2\alpha+3f(\eta)\psi_1'(\eta)+f'(\eta)\psi_1(\eta)=\int_\eta^\infty h(\xi)\,d\xi$$
$$\psi_1(0)=0, \quad \psi_1(\infty)=0 \quad (14)$$

where

$$h(\xi)=[3f''(\xi)\{f(\xi)-\xi f'(\xi)\} + 4\{f'(\xi)\}^2+\xi t'(\xi)/2]\sin 2\alpha.$$

The value of γ in equation (10b) can now be determined by requiring that ϕ of equation (10b) be equal to that of equation (12) as $\eta\to\infty$, i.e.

$$\gamma=\lim_{\eta\to\infty}[-3f(\eta)]. \quad (15)$$

Equations (6) together with the boundary conditions derived above constitute the governing equations for the corner of arbitrary angle. As a simple verification, these equations can be shown to recover the equations in Cartesian coordinates [6] for $\alpha=45°$ by substituting the transformation relations for η and v.

4. METHOD OF SOLUTION

The governing equations (6) subject to the boundary conditions (7), (9), (10) and (12) discussed in the previous section are to be solved for u, Ω, ϕ, ψ and θ in the domain $0\leqslant\eta,\ \zeta\leqslant\infty$. Since the corner-layer variables Ω and ψ become unbounded as $\zeta\to\infty$, we introduce the following variables to make the numerical treatment of the problem more tractable:

$$\bar\Omega=\Omega-\zeta f''(\eta)/\cos\alpha, \quad \bar\psi=\psi-\zeta f'(\eta)\cos\alpha. \quad (16)$$

It is also convenient to transform the unbounded region $(0\leqslant\eta,\ \zeta\leqslant\infty)$ into a finite computational domain $(0\leqslant N,\ S\leqslant 1)$, which can be accomplished by the following simple transformation:

$$N=\frac{a\eta}{1+a\eta}, \quad S=\frac{a\zeta}{1+a\zeta} \quad (17)$$

where a is a grid-spacing parameter. A uniform grid in the computational plane gives a non-uniform grid in the physical plane with the grids being more heavily concentrated near the surface and the symmetry plane.

The equations and the boundary conditions are rewritten in terms of the new variables and are solved by the alternate direction implicit scheme used in ref. [6]. The mesh size, H, and the grid-spacing parameter, a, that were used earlier [6] are found adequate in the present analysis

$$H=0.02, \quad a=0.2.$$

The solution is considered to have converged when the variation in successive iterations becomes less than 10^{-4} as done in ref. [6].

5. RESULTS AND DISCUSSION

In order to assess the accuracy of the procedure including the effect of the obliqueness of the coordinate system, the results for 90° corner flow are compared with the earlier results of ref. [6] (Figs. 2–7). The streamwise velocity component and the temperature are in excellent agreement. The deviation is less than 1% in the relative sense. The crossflow velocity components are also in good agreement except in the regions where the streamwise component u becomes large. Such behaviour may partially be explained if we note that the deviation can be exaggerated by the large values of u (see equations (5)). Although the relative discrepancies in this region reach as large as 4–5%, the absolute values of the crossflow component are still quite small compared to the streamwise component and will not be a concern for the present purposes.

The numerical results are obtained for six corner angles ranging from 60° to 300° for two different Prandtl numbers, 0.72 and 7.0, and are presented in Figs. 2–9. In Fig. 2, the isovels of streamwise velocity u for corner angles of 90° and 270° are depicted. For 90° corner, closed contours of isovels, on which the values of u are greater than the maximum value of the two-dimensional velocity distribution along a vertical plate, appear in the vicinity of the symmetry plane near the corner. The maximum value occurs on the symmetry plane. On the other hand, for 270° corner,

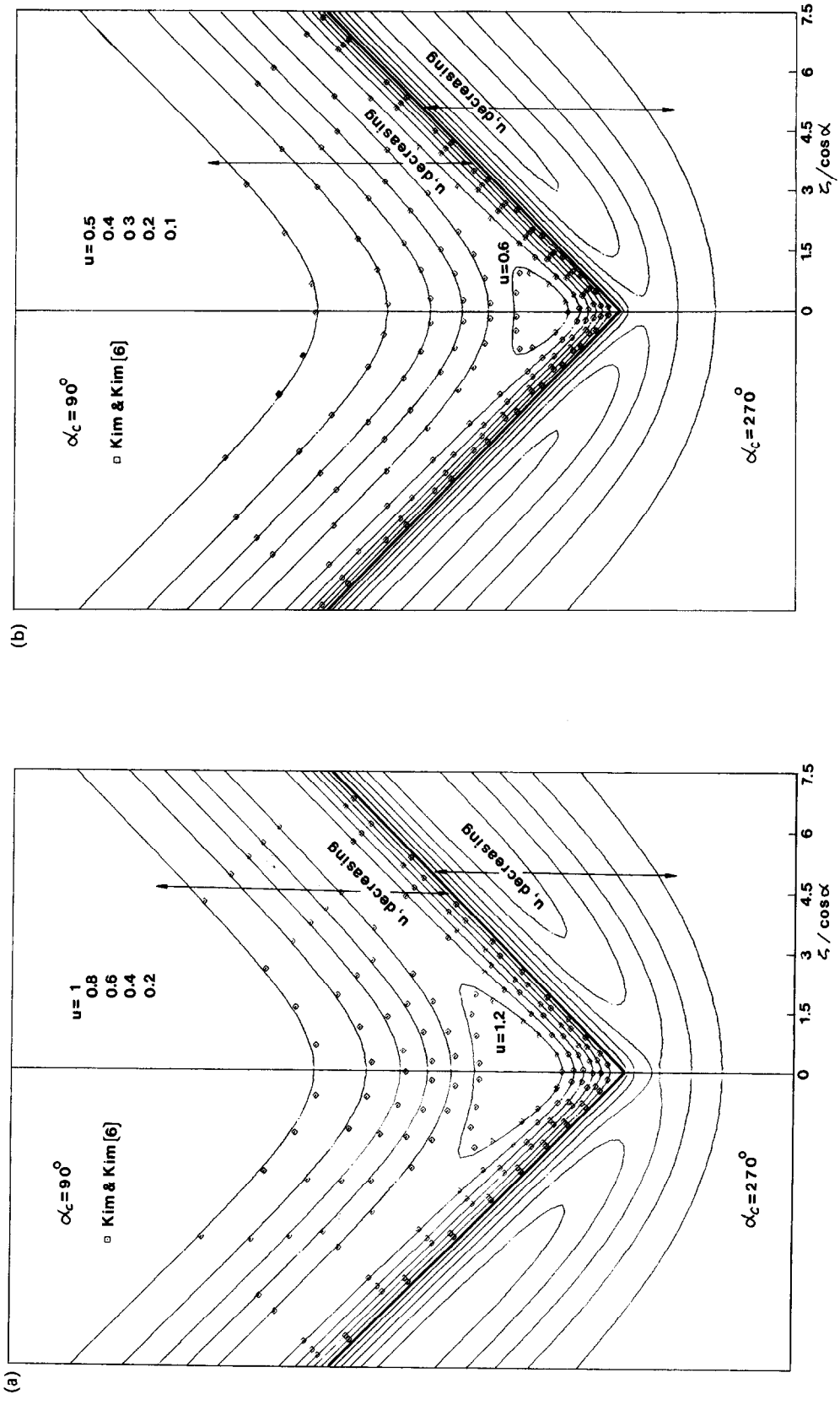

FIG. 2. Streamwise isovels for $\alpha_c = 90^\circ$ and 270°: (a) $Pr = 0.72$; (b) $Pr = 7.0$.

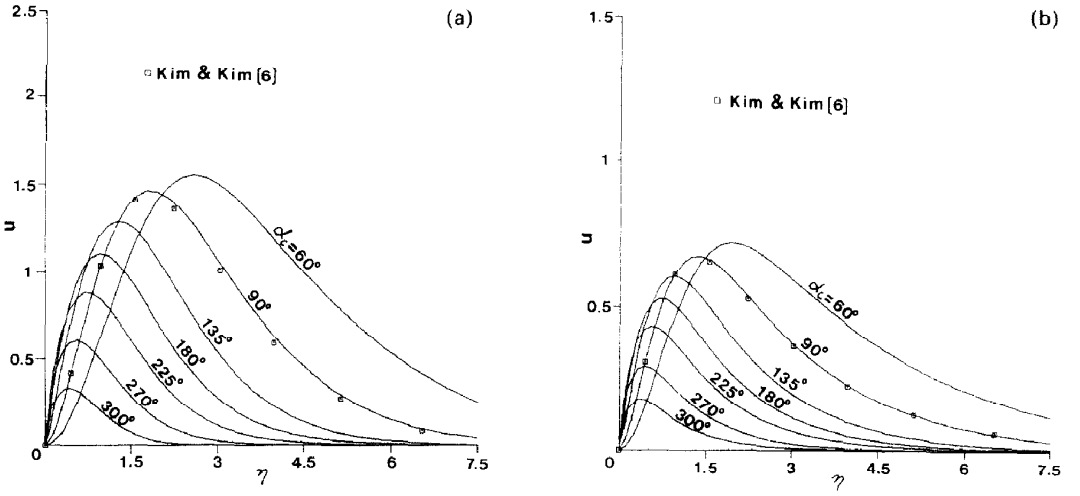

FIG. 3. Streamwise velocity profiles in the symmetry plane for various corner angles: (a) $Pr = 0.72$; (b) $Pr = 7.0$.

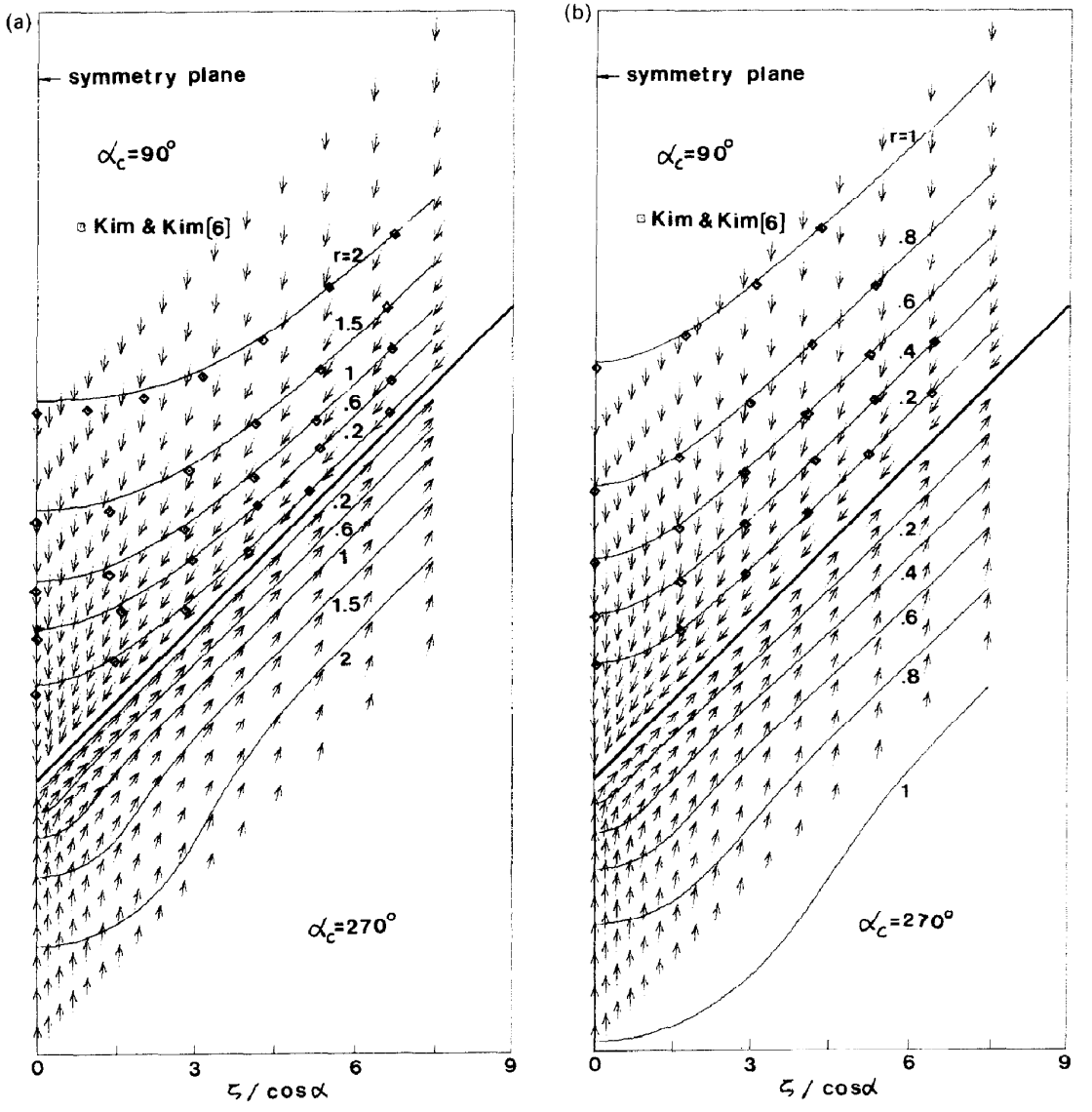

FIG. 4. Magnitudes and directions of crossflow for $\alpha_c = 90$ and 270 : (a) $Pr = 0.72$; (b) $Pr = 7.0$.

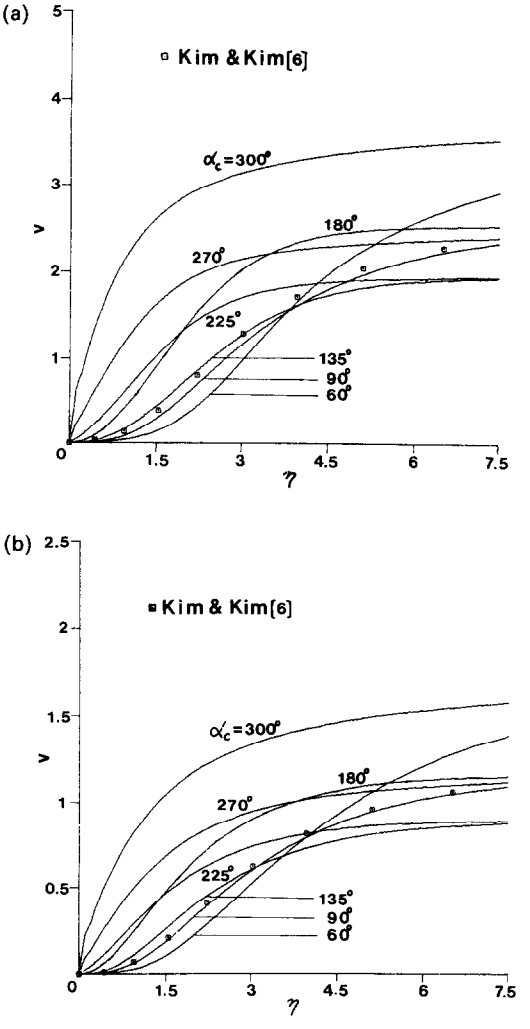

FIG. 5. Crossflow profiles in the symmetry plane for various corner angles: (a) $Pr = 0.72$; (b) $Pr = 7.0$.

no closed contour of streamwise isovels appears, and the maximum value of the streamwise velocity on the symmetry plane is smaller than the corresponding two-dimensional one (see also Fig. 3). For 90° (270°) corner, the velocity–boundary-layer thickness has its maximum (minimum) value at the symmetry plane and becomes thinner (thicker) as ζ increases and ultimately approaches its asymptotic two-dimensional value. The qualitative features of streamwise velocity distributions for corner angles $\alpha_c < 180°$ ($\alpha_c > 180°$) are the same as those for 90° (270°). To complement Fig. 2, Fig. 3 shows the effect of the corner angle on the streamwise velocity profile in the symmetry plane for angles in the range of 60°–300°. The thickness of the velocity boundary layer as measured in the symmetry plane is increasing as the corner angle is reduced: the maximum value of u becomes larger and the point of its occurrence moves outward.

Figure 4 shows the isolines of the magnitude of the scaled crossflow r, and the direction for corner angles 90° and 270°. The magnitude of the crossflow increases with the distance from the corner and decreases with the Prandtl number. The crossflow for $\alpha_c = 90°$ (generally for $\alpha_c < 180°$) is directing almost radially inward to the corner, while for $\alpha_c = 270°$ (generally for $\alpha_c > 180°$) inward flow toward the corner occurs only in the vicinity of the symmetry plane and the fluid near the wall diverges outward. Unlike high-Reynolds-number flows [9], no complicated swirling motion is observed. This simple inward/inward and outward behaviour of the crossflow explains the increases/decreases of the streamwise velocity components discussed above. In Fig. 5, profiles of the crossflow velocity component v in the symmetry plane are shown for corner angles ranging from 60° to 300°. The profiles show regular and expected behaviours. It is to be noted that the profiles for corner angles α_c and $2\pi - \alpha_c$ algebraically approach the same limit as $\eta \to \infty$.

The isotherms for corner angles 90° and 270° are shown in Fig. 6. The temperature profiles in the symmetry plane are depicted in Fig. 7 for various corner angles. The thickness of the thermal boundary layer as measured in the symmetry plane decreases as the corner angle increases. It is interesting to note that the temperature close to the corner varies more slowly as the corner angle becomes smaller; there appears to be a point of inflection in the profile when $\alpha_c < 180°$. The ratio of the thermal to the velocity boundary-layer thickness decreases with the Prandtl number as expected from the two-dimensional natural convection.

Figure 8 shows the local Nusselt number Nu

$$Nu = -\frac{\theta_\eta(0,\zeta)}{\cos\alpha}\left(\frac{Gr}{4}\right)^{1/4}. \tag{18}$$

For a fixed ζ, the Nusselt number becomes larger as the corner angle increases. It increases (decreases) monotonically for $\alpha_c < 180°$ (for $\alpha_c > 180°$) from zero (from infinity) to the asymptotic two-dimensional value as ζ increases. By contrast, for the case of forced convection along a corner [12], Nu attains the maximum (minimum) value and then approaches the two-dimensional value. The difference in the behaviour of Nu distributions between the natural and the forced convections can mainly be attributed to the different behaviour of the crossflow.

In Fig. 9, the results for the wall shear stress for $60° \leqslant \alpha_c \leqslant 300°$ are shown. The shear stress τ_w is approximately given by, neglecting the effect of the crossflow

$$\tau_w = \frac{u_\eta(0,\zeta)}{\cos\alpha}\frac{\tau_{w\infty}}{f''(0)} \tag{19}$$

where $\tau_{w\infty}$ is the value of τ_w as $\zeta \to \infty$

$$\tau_{w\infty} = \frac{\rho\nu^2}{x^2} f''(0)\left(\frac{Gr}{4}\right)^{3/4}.$$

It is observed from the figure that for $\alpha_c < 180°$, τ_w starts from zero at the corner but attains the maximum value before it gradually falls back to its asymptotic

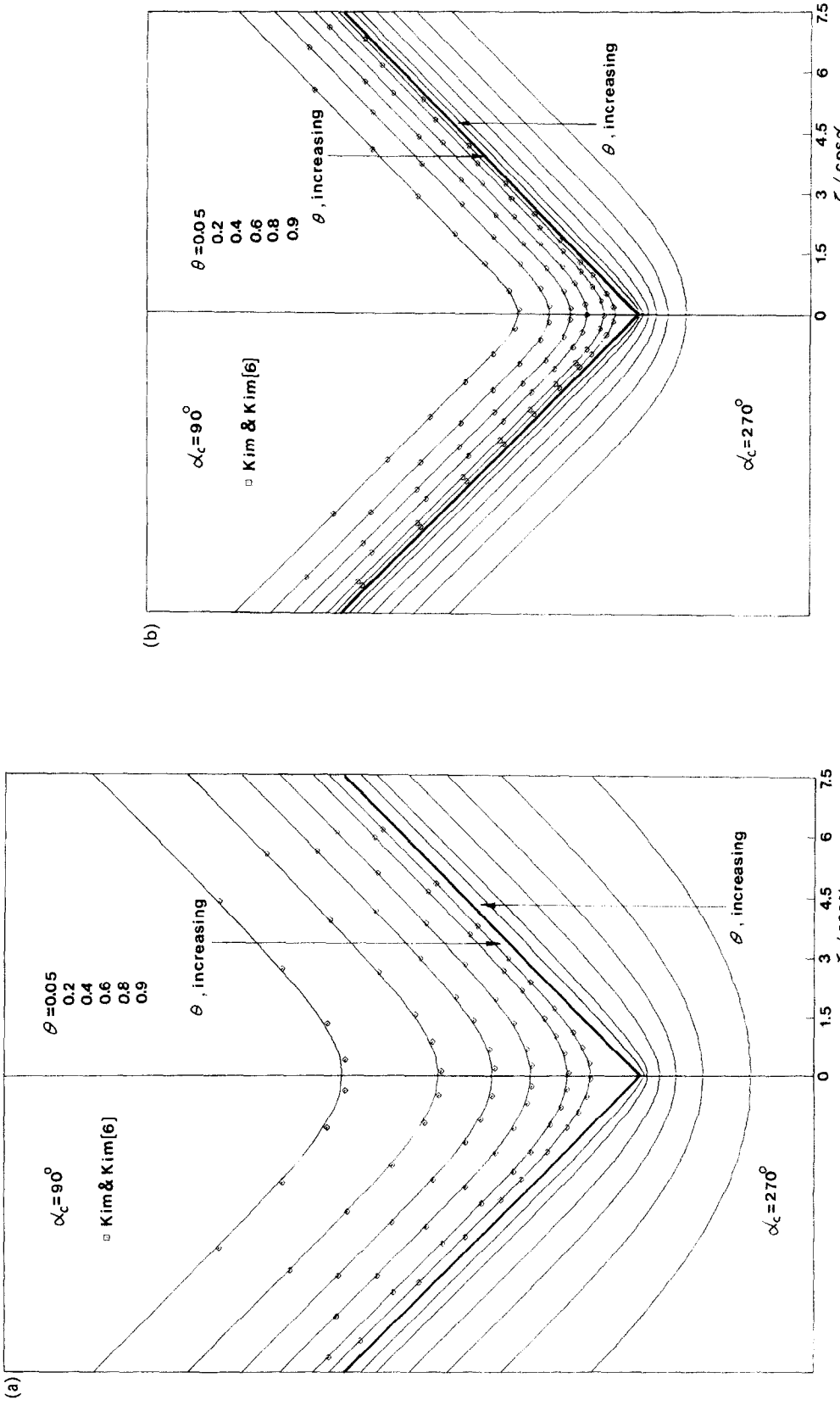

FIG. 6. Isotherms for $\alpha_c = 90$ and 270 : (a) $Pr = 0.72$; (b) $Pr = 7.0$.

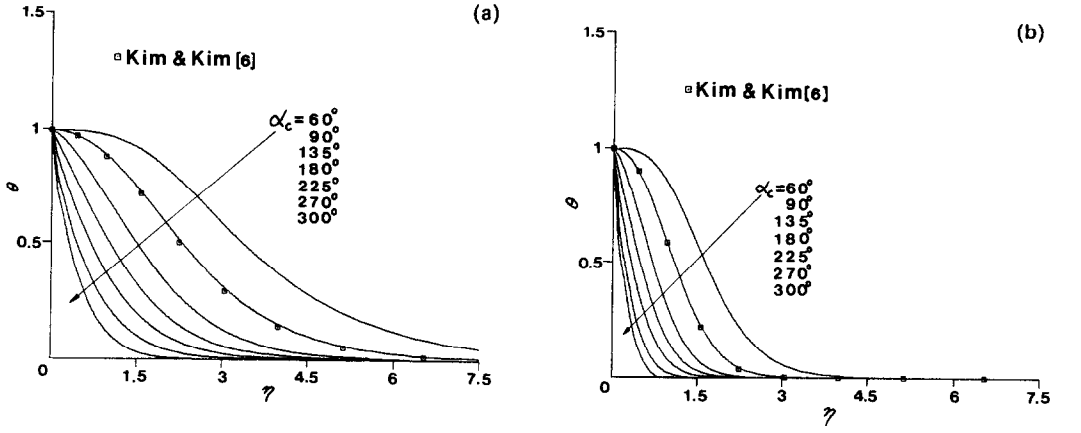

FIG. 7. Temperature profiles in the symmetry plane for various corner angles: (a) $Pr = 0.72$; (b) $Pr = 7.0$.

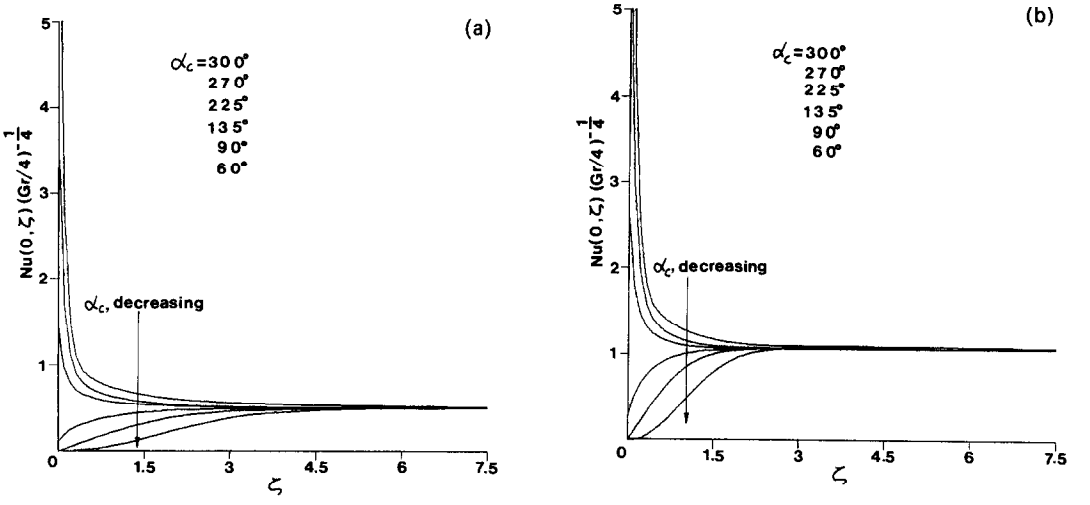

FIG. 8. Local Nusselt number distributions for various corner angles: (a) $Pr = 0.72$; (b) $Pr = 7.0$.

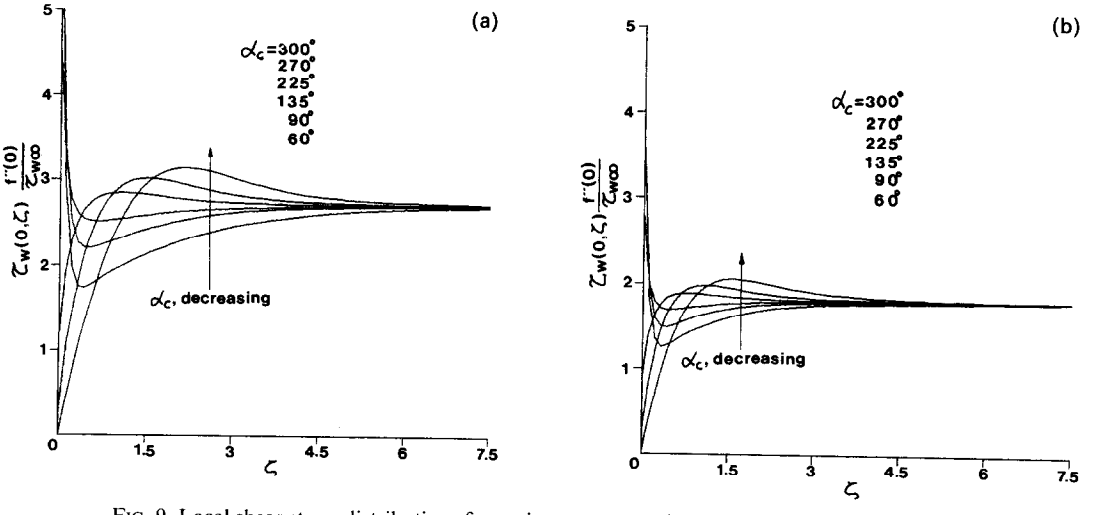

FIG. 9. Local shear stress distributions for various corner angles: (a) $Pr = 0.72$; (b) $Pr = 7.0$.

two-dimensional value as $\zeta \to \infty$. This can be expected physically. As seen in Fig. 3, as the corner is approached, the streamwise velocity increases by the enhanced entrainment due to the interaction of boundary layers and so does the shear stress. However, in the close neighbourhood of the corner, the increased momentum is counterbalanced and eventually overwhelmed by the compound viscous effect of both walls. The shear stress decreases accordingly. For $\alpha_c > 180^\circ$, τ_w rises to rather large values as $\zeta \to 0$, decreases to its minimum value and then increases to the two-dimensional value with the increase of ζ. It is also observed from the figure that, for $\alpha_c < 180^\circ$, τ_w is larger (smaller for $\alpha_c > 180^\circ$) for the greater corner angle near the corner but the trend reverses beyond the point where τ_w has the peak value.

From the numerical results shown in Figs. 2–9, it is seen that the qualitative features of fluid motion and heat transfer near the corner are entirely different if the corner angle α_c is greater than or less than 180°. Contrasting behaviours in the crossflow pattern and consequently the Nusselt number distribution near the corner are also noted between the present results and those of the forced convection in the high-Reynolds-number flow.

REFERENCES

1. F. Restrepo and L. R. Glicksman, The effect of edge conditions on natural convection from a horizontal plate, *Int. J. Heat Mass Transfer* **17**, 135–142 (1974).
2. R. Eichhorn and M. M. Hasen, Mixed convection about a vertical surface in crossflow: a similarity solution, *ASME J. Heat Transfer* **102**, 775–777 (1980).
3. D. W. Hartfield and D. K. Edwards, Edge and aspect ratio effects on natural convection from the horizontal heated plate facing downwards, *Int. J. Heat Mass Transfer* **24**, 1019–1024 (1981).
4. J. M. Merkin and F. T. Smith, Free convection boundary layer near corner and sharp trailing edges, *ZAMP* **33**, 36–52 (1982).
5. C. Y. Liu and A. C. Guerra, Free convection in a porous medium near the corner of arbitrary angle formed by two vertical plates, *Int. Commun. Heat Mass Transfer* **12**, 431–444 (1985).
6. M. H. Kim and M.-U. Kim, Natural convection near a rectangular corner, *Int. J. Heat Mass Transfer* **31**, 1357–1364 (1988).
7. S. G. Rubin and B. Grossman, Viscous flow along a corner: numerical solution of the corner layer equations, *Q. Appl. Math.* **29**, 169–186 (1971).
8. K. N. Ghia, Incompressible streamwise flow along an unbounded corner, *AIAA J.* **13**, 902–907 (1975).
9. W. H. Barclay and A. H. Ridha, Flow in streamwise corners of arbitrary angle, *AIAA J.* **18**, 1413–1420 (1980).
10. S. G. Rubin, Incompressible flow along a corner, *J. Fluid Mech.* **26**, 97–110 (1966).
11. A. Pal and S. G. Rubin, Asymptotic features of viscous flow along a corner, *Q. Appl. Math.* **29**, 91–108 (1971).
12. M. H. Kim, M.-U. Kim and D. H. Choi, Forced convective heat transfer in the flow along a corner of arbitrary angle, *Mech. Res. Commun.* **15**, 269–274 (1988).

CONVECTION NATURELLE PROCHE D'UN COIN VERTICAL D'ANGLE QUELCONQUE

Résumé—On présente la convection thermique naturelle laminaire près d'un coin vertical d'angle quelconque. Pour des grands nombres de Grashof, les équations et les conditions aux limites sont formulées dans un système de coordonnées obliques, basé sur la méthode des développements asymptotiques. L'analyse est valable pour des angles autres que 0° et 360°. Les distributions de vitesse et de température sont numériquement déterminées en utilisant la technique aux différences finies du type ADI pour des angles allant de 60° à 300° et pour des nombres de Prandtl de 0,72 et 7,0.

NATÜRLICHE KONVEKTION IN DER NÄHE EINER VERTIKALEN ECKE BELIEBIGEN WINKELS

Zusammenfassung—Es wird der Wärmeübergang bei laminarer natürlicher Konvektion in der Nähe einer vertikalen Ecke beliebigen Winkels untersucht. Die Grenzschichtgleichungen in der Ecke und die geeigneten Randbedingungen werden für große Grashof-Zahlen in einem schiefwinkligen Koordinatensystem beschrieben, das auf der Methode angepaßter asymptotischer Entwicklungen beruht. Die Untersuchung ist für jeden beliebigen Winkel gültig, mit Ausnahme der Grenzwinkel 0° und 360°. Die Geschwindigkeits- und Temperaturverteilungen werden numerisch mit Hilfe der Methode der finiten Differenzen (mit ADI) ermittelt, und zwar für Eckwinkel von 60° bis 300°, bei Prandtl-Zahlen von 0,72 und 7,0.

ЕСТЕСТВЕННАЯ КОНВЕКЦИЯ ВБЛИЗИ ВЕРТИКАЛЬНОГО УГЛА ПРОИЗВОЛЬНОЙ ВЕЛИЧИНЫ

Аннотация—Исследуется ламинарный естественноконвективный теплоперенос вблизи вершины вертикального угла произвольной величины. При небольших числах Грасгофа уравнения для этой задачи и соответствующие граничные условия формулируются в системе косоугольных координат на основании метода сращиваемых асимптотических расложений. Анализ является справедливым при любой величине угла за исключением предельных, составляющих 0° и 360°. С использованием неявного метода переменных направлений численно определяются распределения скоростей и температур для углов, изменяющихся от 60° до 300° при числах Прандтля 0,72 и 7,0.